Class II histone deacetylases are directly recruited by BCL6 transcriptional repressor.

Claudie Lemercier, Marie-Paule Brocard, Francine Puvion-Dutilleul, Hung-Ying Kao, Olivier Albagli, Saadi Khochbin

J. Biol. Chem., Vol. 277, Issue 24, 22045-22052, June 14, 2002

Class II Histone Deacetylases Are Directly Recruited by BCL6 Transcriptional Repressor*

Claudie Lemercier‡, Marie-Paule Brocard‡, Francine Puvion-Dutilleul§, Hung-Ying Kao¶‖, Olivier Albagli§‡‡, and Saadi Khochbin‡**§§**

From the ‡ INSERM U309, Equipe Chromatine et Expression des Gènes, Institut Albert Bonniot, Domaine de la Merci, 38706 La Tronche Cedex, France, the § CNRS UPR 1983, 7 rue Guy Môquet, BP 8, 94801 Villejuif Cedex, France, and the ¶ Department of Biochemistry, School of Medicine, Case Western Reserve University, the Research Institute of University Hospitals of Cleveland and the Comprehensive Cancer Center of Case Western Reserve University and University Hospitals of Cleveland, Cleveland, Ohio 44106

Received for publication, February 20, 2002, and in revised form, March 28, 2002

Abstract

BCL6 is a member of the POZ/zinc finger (POK) family involved in survival and/or differentiation of a number of cell types and in B cell lymphoma upon chromosomal alteration. Transcriptional repression by BCL6 is thought to be achieved in part by recruiting a repressor complex containing two class I histone deacetylases (HDACs). In this study we investigated whether BCL6 could also target members of class II HDACs. Our results indicate that three related class II deacetylases, HDAC4, HDAC5, and HDAC7 can associate with BCL6 *in vivo* and *in vitro*. Using electron microscopy, we found that endogenous BCL6 and class II HDACs partially co-localize in the nucleus. Overexpression experiments showed that BCL6 and HDAC4, -5, or -7 are intermingled onto common nuclear substructures and form stable complexes. A highly conserved domain in the N-terminal region of HDAC5 and HDAC7 as well as the zinc finger region of BCL6 were found necessary for the complex formation *in vivo* and *in vitro*. Moreover, our data point to the zinc finger region of BCL6 as a multifunctional domain which, beside its known capacity to bind DNA, is involved in the nuclear targeting of the protein and in the recruitment of the class II HDACs, and hence constitutes an autonomous repressor domain. Since PLZF, a BCL6 relative, could also interact with HDAC4, -5, and 7, we suggest that class II HDACs are largely involved in the control of the POK transcription factors activity.

Introduction

The presence of an N-terminal BTB/POZ (bric à brac, tramtrack, broad complex/pox virus, and zinc finger) domain and C-terminal C2-H2 zinc finger(s) defines the family of POK ((BTB/)POZ and *krüppel*-like zinc finger) proteins found in both vertebrates and *Drosophila*. POK proteins are sequence-specific DNA-binding transcription factors, some of them being involved in human oncogenesis. For instance, non-Hodgkin lymphomas are often associated with the structural alteration, and presumably mis-regulation, of the *BCL6* (also named *LAZ3*) gene encoding a six-zinc finger POK protein (1, 2). Moreover, a few cases of acute promyelocytic leukemia are associated with the t(11;17) reciprocal translocation that fuses the retinoic acid receptor α to PLZF, a nine-zinc finger POK protein. Finally, other POK proteins,

such as HIC-1 (3, 4) and APM-1 (5) have been proposed to act as tumor suppressors in different human malignancies.

BCL6 regulates at least lymphocyte (6, 7), myocyte (8, 9), male germ cells (10), and possibly keratinocyte survival and/or differentiation (11). Recently, a set of BCL6 potential target genes has been identified by DNA microarray screening in lymphocytes. BCL6 was found to repress a number of genes involved in B cell activation and terminal differentiation, inflammation, and cell cycle regulation (12). Earlier studies have shaded light on the molecular mechanisms by which BCL6 negatively regulates gene transcription. BCL6 recruits, through multiple contacts, a repressor complex containing both silencing mediator of retinoid and thyroid receptors or its close relative nuclear receptor co-repressor, two vertebrate homologues of the yeast repressor SIN3 (mSINA/B), and two related class I histone deacetylases, HDAC1[1] and HDAC2 (13-20). However, these co-repressors do not explain all the regulatory properties of the POK proteins. In fact, it appears that POK transcriptional repressors are capable of recruiting other co-repressors. Indeed, C-terminal binding protein might interact with *Drosophila* TTK (21), whereas another unrelated co-repressor, termed B-CoR, specifically binds to BCL6 in a silencing mediator of retinoid and thyroid receptors/nuclear receptor co-repressor mutually exclusive manner (22).

Whereas class I deacetylases (HDAC1,-2, -3, and -8) are closely related to the yeast *rpd3* gene product, other HDACs (HDAC4, -5, -6, -7, -9, and -10) have been characterized in vertebrates, and collectively referred to as class II HDACs. HDAC4, -5, -7, and -9 share two regions, each encompassing half of the protein: a C-terminal catalytic domain resembling that of the yeast HDA1 deacetylase and a N-terminal "regulatory" domain (23-26). The organization of HDAC6 and HDAC10 is atypical. Indeed, both HDAC6 and HDAC10 harbor two regions of homology with the class II catalytic domain (23, 24, 27-29). However, whereas HDAC6 contains two active catalytic domains (24), the second catalytic domain-like region of HDAC10 does not appear to be active (29). Another feature of all of the class II members is their ability to shuttle in a regulated fashion between the nucleus and the cytoplasm (see Ref. 30 for review).

The role of class II HDACs in the control of transcription is believed to be important but is only beginning to be analyzed. In particular, although class I and class II HDACs represent two structurally distinguishable families, their functional relationship, beyond their common ability to deacetylate histone *in vitro*, remains largely unknown. In this study, we investigated whether POK proteins, such as BCL6, could also associate with class II histone deacetylases. Our data showed that indeed HDAC4, -5, and -7 are recruited by BCL6 *in vivo* and *in vitro*. Together with previously published data, these findings indicate that BCL6, as well as other POK proteins, directly and indirectly recruit both class I and class II HDACs.

Materials and Methods

DNA Constructs-- pcDNA-HA-HDAC5 and HA-HDAC4 (31) and pcDNA-HA-HDAC7 (25) have been described before. HDAC5, HDAC4, and HDAC7 deletion fragments were constructed by PCR using the high Fidelity *Taq*/Pwo polymerases mixture (Roche Molecular Biochemcials) and cloned in-frame into pGEX5 plamids (Amersham Biosciences). Human BCL6 (LAZ3) cDNA encoding the full-length protein (1-706) or deletion fragments (encoding amino acids 132-706, 501-706, 132-519, 1-626, 1-573, and 1-519) were amplified by PCR from the pTL-LAZ3 plasmid (13) without the Flag tag, and subsequently cloned into pcDNA3.1 plasmid (Invitrogen). Gal4 DNA-binding fusion protein were obtained by

subcloning BCL6 fragments into pcDNA-Gal4 DB vector (32). L8G5-Luc and L8-Luc reporter plasmids containing 8 LexA operators with 5 Gal4-binding sites or without Gal4 sites, respectively, as well as the LexA-VP16 activator plasmid (31, 32), have been described before. The SV40-based PLZF expression vector (pSG5-PLZF) is a generous gift of Dr. Koken (33). For producing the proteins in baculovirus, BCL6 cDNA encoding the zinc finger region (amino acids 501-706) was cloned into the pBacPAK9 vector (CLONTECH), in-frame with a histidine tag at the C terminus.

Antibodies-- The antibodies used were: anti-BCL6 N3 or C19 rabbit antibodies (Santa Cruz Biotechnology) or anti-Flag M2 mouse antibody (Sigma-Aldrich) to detect BCL6; anti-HA Y11 rabbit antibody (Santa-Cruz Biotechnology) or 3F10 anti-HA rat antibody (Roche Molecular Biochemicals) to detect the HA-tagged transfected HDACs; anti-HDAC4 N18 and anti-HDAC5 P16 goat polyclonal antibodies (Santa Cruz Biotechnology) to detect endogenous class II HDACs; anti-PLZF mouse antibody (33) and anti-Gal4DB (RK5C1, Santa Cruz). For ultrastructural studies in UTA-L cells, secondary antibodies were gold-labeled goat anti-rabbit immunoglobulin (IgG) and goat anti-mouse IgG (British Biocell International Ltd., Cardiff, United Kingdom).

Cell Culture, Transfections, and Reporter Gene Assays-- Human U2OS osteosarcoma-derived UTA-L (34) cells and human lung carcinoma A549 cells were grown in "growth medium," that is a 50/50 mixture of Dulbecco's modified Eagle's/Ham's F-12 medium (Invitrogen) containing 10% fetal calf serum (Sigma-Aldrich) and antibiotics. For UTA-L cells, growth medium was supplemented with tetracycline (Sigma-Aldrich, 2 μg/ml), G418 (Invitrogen, 500 μg/ml), and puromycine (Sigma-Aldrich, 1 μg/ml). To induce BCL6 expression, UTA-L cells were rinsed twice with growth medium, then trypsinized, centrifuged, and plated in growth medium. Transfections of both UTA-L and C2 cells were performed using 1.5 μg of the appropriate expression vector(s) and 3 μl of FuGENE 6 (Roche Molecular Biochemicals) according to the supplier's instructions. Induction of BCL6 expression in UTA-L cells was performed 24 h before transfection with any transiently transfected HDACs. Note that the expression of BCL6 continues during the transfection and the subsequent culture, as these steps are also performed in a tetracycline-free medium. HeLa cells were grown in a standard growth medium (Dulbecco's modified Eagle's, 10% fetal calf serum, 2 mM L-glutamine, and antibiotics) and transfected as described before (31). Typically, 20 ng of pcDNA-Gal4 DB plasmids, 400 ng of L8G5-Luc or L8-luc reporter plasmid, 100 ng of LexA-VP16 activator plasmid, and 100 ng of pCMV-β (CLONTECH) were used in each transfection. Cells extracts were prepared 24 h post-transfection and processed for luciferase (Luciferase Assay System, Promega) and β-galactosidase (Luminescent β-gal detection kit, CLONTECH) assays. Luciferase units were normalized according to the β-galactosidase values.

Immunofluorescence and Confocal Microscopy Analyses-- Immunofluorescence analyses were performed as previously described (34). Briefly, 24 h after transfection, cells on a 3.5-cm dishes were rinsed with PBS, fixed in formaline (Sigma-Aldrich) for 10 min, washed in PBS, permeabilized in a 0.25% Triton, 50 mM NH_4Cl solution in PBS for 10 min, rinsed in PBS, and exposed for 1 h at room temperature to the primary antibodies diluted at 1/100 in a PBS, 0.2% gelatin solution (except for M2 anti-Flag which was diluted at 1/800). Cells were then rinsed in PBS, 0.2% gelatin and exposed to the appropriate secondary antibodies, all were purchased from Molecular Probes: goat anti-rabbit Alexa 488 plus goat anti-mouse Alexa 594 (Figs. 2*B* and 5*C*) and goat anti-rat Alexa 488 plus goat anti-rabbit Alexa 594 (Fig. 6*E*). The dishes were then rinsed with PBS and mounted in Mowiol (Merck) to be analyzed by a

laser scanning microscope (Leica) using a ×63 objective. The images were finally processed with Adobe photoshop.

Electron Microscopy-- Non-induced and 24-h induced UTA-L cell cultures were transfected with an expression vector encoding the desired HDAC and prepared for electron microscopy as previously described (35). Briefly, cell cultures were fixed 24 h after transfection with formaldehyde, dehydrated in methanol, and embedded in Lowicryl K4M. Ultrathin sections were collected on Formvar carbon-coated gold grids. For the detection of the overexpressed HDACs (in UTA-L cells), grids were incubated in the presence of the Y11 anti-HA antibody (at 1/10 dilution in PBS for 1 h) and anti-rabbit IgG conjugated to 10-nm gold particles (at 1/25 dilution in PBS for 30 min), successively, prior to being stained with either uranyl acetate alone or by the EDTA regressive staining method, which preferentially bleaches the condensed chromatin. BCL6 was detected either with the C19 anti-BCL6 or M2 anti-Flag antibodies. For the simultaneous detection of overexpressed BCL6 and HDACs (in UTA-L cells), grids were floated for 1 h on a mixture of the M2 anti-Flag and Y11 anti-HA antibodies, each at 1/10 dilution in PBS, then for 30 min over a mixture of anti-mouse IgG and anti-rabbit IgG conjugated to gold particles of different size (5 and 10 nm). Co-detection of the endogenous BCL6 and either HDAC4 or HDAC5 was performed on human A549 cells and mouse C2 cells as follows. Grids were incubated successively with BCL6 C19 antibody (1/10 in PBS for 1 h), HDAC4 (N18) antibody (1/10 in PBS), HDAC5 (P16) antibody (1/10 in PBS), and finally, a mixture of gold-labeled antibodies consisting of 6-nm donkey anti-rabbit antibody and 12-nm donkey anti-goat antibody (Jackson Immunoresearch Laboratories, Inc., West Grove, PA), each diluted 1/20 in PBS with 1% bovine serum albumin and 1% Triton X-100.

Electrophoretic Mobility Shift Assays-- Electrophoretic mobility shift assays were performed essentially as described before (32) except that the gels were prepared and run in 0.5 × TBE (44.5 mM Tris-HCl, pH 8.0, 44.5 mM boric acid, 1 mM EDTA). Oligonucleotides were end-labeled with [γ-^{32}P]ATP and T4 polynucleotide kinase. After removal of unincorporated nucleotides, the sense and antisense strands were annealed and used as a probe. The 20-bp BCL6-binding site used in this study (5'-GAAAATTCCTAGAAAGCATA-3') was described before (36).

Co-immunoprecipitation and Western Blotting-- Cell extracts were prepared from frozen pellets of UTA-L cells co-transfected with pcDNA-HA-HDAC5 (or HA-HDAC4 or HA-HDAC7) and pcDNA-BCL6 or pcDNA3 empty vector. Proteins were extracted in 0.5% Nonidet P-40, 20 mM Tris-HCl, pH 8, 150 mM NaCl, 1 mM phenylmethylsulfonyl fluoride, 10% glycerol, 1 mM EDTA for 20 min on ice. Cell debris was removed by centrifugation for 10 min at 12,000 × *g* and the soluble material was submitted to immunoprecipitation with the C19 anti-BCL6 polyclonal antibody for 1 h at 4 °C. The immune complexes were precipitated with Sepharose-protein G (Amersham Biosciences) for an additional hour at 4 °C. After four washes in lysis buffer and two in PBS, the bound proteins were eluted in SDS-PAGE sample buffer and analyzed by Western blotting. Blots were subsequently probed with primary antibodies (C19 anti-BCL6 or 3F10 anti-HA antibodies) and secondary antibodies conjugated to peroxidase, before being detected by chemiluminescence (ECL+, Amersham Biosciences).

In Vitro Protein-Protein Interaction Assays-- *In vitro* translated proteins were produced from pcDNA3 plasmids using T7 RNA polymerase, [^{35}S]methionine (ICN), and the TNT rabbit reticulocyte lysate system (Promega). GST fusion proteins were produced in *Escherichia coli* BL21 upon isopropyl-1-thio-β-D-galactopyranoside induction and purified using glutathione-

agarose beads according to the supplier's instructions (Amersham Bioscience). GST pull-down assays were performed essentially as described before (31). For direct protein interaction, the BCL6 zinc finger region (amino acids 501-706) fused to a histidine tag was produced in baculovirus using the BacPAK Baculovirus Expression System (CLONTECH). The protein was then purified from insect cell extracts by nickel affinity column (Ni-NTA-agarose, Qiagen), eluted with 250 mM imidazole and finally dialyzed against 20 mM Tris-HCl, pH 7.5, 10% glycerol, and 1 mM dithiothreitol. The purified protein was used in GST pull-down experiments as above and bound BCL6 was detected by Western blot with C19 anti-BCL6 antibody.

Results

Partial Association of Endogenous BCL6 and Class II HDACs-- In a first attempt to examine whether BCL6 and class II HDACs could associate *in vivo*, we used immunogold labeling and electron microscopy (EM) to co-detect these proteins in human A549 lung cells which express endogenous BCL6, HDAC4, and HDAC5 mRNA (data not shown). EM analyses indicated that endogenous HDAC4 or endogenous HDAC5 (12 nm gold particles) as well as endogenous BCL6 (6 nm-gold particles) were detected as individual foci in the nucleus of these cells (Fig. 1, *A*, *B*, *D*, and *E*). Interestingly, some clusters showed an association or juxtaposition between the endogenous BCL6 and either endogenous HDAC4 (Fig. 1, *A* and *B*, *arrow*) or endogenous HDAC5 (Fig. 1*E*, *arrow*). These data indicate that HDAC4 and HDAC5 molecules are entrapped within or juxtaposed to some foci of BCL6 in A549 cells. Note, however, that this co-localization is partial as our results also showed that class II HDACs and BCL6 can also be independently engaged into distinct complexes in these cells (Fig. 1*D*). In mouse C2 myocytes, which also express BCL6 and class II HDACs (Ref. 8 and data not shown; see also, Refs. 37-39), a similar partial co-localization was observed between endogenous BCL6 and endogenous HDAC4 (Fig. 1*C* and data not shown). We conclude that, at physiological levels of expression, a fraction of the class II HDAC molecules are associated with BCL6 in at least two cell lines.

Co-localization of BCL6 with HDAC4, -5, and -7 in a BCL6-inducible Cell Line-- To search for a potential interaction between BCL6 and class II HDACs and because of their low expression level in various cell lines, we next used a cell line stably transfected with an inducible BCL6 expression vector (UTA-L cells). In these cells a flagged-version of BCL6 is under the control of a tetracycline-sensitive promoter (34). Upon tetracycline removal, BCL6 protein expression is induced within 24 h as shown on Fig. 2*A*, and is functional as revealed by electrophoretic mobility shift assays using a BCL6-target sequence (Fig. 2*B*).

We next examined the subcellular distribution of BCL6 and class II HDACs. To this end, induced (BCL6 expressing) UTA-L cells were transiently transfected with a vector encoding HA-tagged HDAC4, -5, or -7, and subcellular localization of these proteins was analyzed by scanning confocal microscopy. In the three cases, we observed a nearly complete coincidence between the two stainings. In almost all the HDAC4-transfected cells, both proteins were found to co-localize onto typical BCL6 nuclear bodies (Fig. 2*C*, *top*), whereas a few cells also displayed co-staining onto cytoplasmic inclusions (data not shown). When HDAC5 and BCL6 were co-expressed, the two proteins were concentrated onto common nuclear subdomains (Fig. 2*C*, *middle*). Finally co-expression of HDAC7 and BCL6 also showed a complete co-localization between the two proteins (Fig. 2*C*, *bottom*).

We next confirmed and refined these findings upon EM. Indeed, HA-HDAC4 could be detected in cytoplasmic inclusions (Fig. 3*A*, *double star*) as well as in, and sometimes around, typical BCL6 nuclear bodies (Fig. 3, *A* and *B*, *star*). In the presence of BCL6 (Fig. 3*C*), HDAC5 (*arrows*) was also present, both in the BCL6 bodies (*star*) and in their interior. Upon higher HDAC5 expression (Fig. 3*D* and data not shown), both HDAC5 and BCL6 stainings were co-distributed within nuclear inclusions (*double star*) indistinguishable from those formed when HDAC5 was expressed alone. In such nuclei, BCL6 bodies (*star*) were found enclosed within HDAC5 nuclear inclusions and both structures were intensely co-labeled with the anti-Flag and anti-HA antibodies (Fig. 3*D*). Finally, both HDAC7 and BCL6 proteins also co-localized either onto "free" BCL6 bodies (*star*, Fig. 3*E*) or onto BCL6 bodies (*stars*) embedded within larger nuclear inclusions (*double star*) also containing both proteins (Fig. 3*F* and data not shown).

In summary, when overexpressed with BCL6, the nuclear fraction of HDAC4, -5, and -7 was primarily targeted to BCL6 bodies. Upon higher expression levels, HDAC5 and HDAC7 formed nuclear inclusions, each presumably arising from a BCL6 body and fusing with each other to form larger inclusions containing both BCL6 bodies as well as dispersed BCL6 molecules.

BCL6 and Class II HDACs Form Stable Complexes in Vivo-- The association between BCL6 and class II HDACs staining observed by both confocal and electron microscope analyzes suggested that they could form stable complexes *in vivo*. To directly test this hypothesis, we transiently co-transfected HA-HDAC4 or -5 or -7 with BCL6 in non-induced UTA-L cells. An anti-BCL6 antibody was then used to immunoprecipitate BCL6-containing complexes, and the potential presence of associated HA-tagged HDACs was examined. Western blot analysis of the immunoprecipitated materials, using an anti-HA antibody, showed that the three HA-HDACs were co-immunoprecipitated with BCL6, indicating that they are capable of forming a stable complex with BCL6 *in vivo* (Fig. 4, *HDAC5 panel*, *lane 4*; *HDAC4 panel*, *lane 8*, and *HDAC7 panel*, *lane 12*). Under the same conditions, when expressed alone, neither of the three HA-HDACs was immunoprecipitated with the anti-BCL6 antibody (Fig. 4, *HDAC5*, *-4*, and *-7 panels*, *lanes 3*, *7*, and *11*, respectively). Moreover, parallel co-immunoprecipitation with an irrelevant antibody (anti-Gal4) failed to show the presence of any of the three HDACs (data not shown). We conclude that class II HDACs not only co-localize with BCL6, but are also capable of forming stable complexes with this transcription factor *in vivo*.

Delineation of the BCL6-binding Site on HDAC5 and HDAC7-- To precisely determine the region involved in the interaction between the class II HDACs and BCL6, a GST pull-down approach was undertaken.

Different fragments of HDAC5 were fused to GST (Fig. 5*A*), and the respective purified proteins were used to monitor their ability to interact with *in vitro* translated ^{35}S-labeled BCL6. A fragment of HDAC5 containing most of the N-terminal non-deacetylase region of the protein (amino acids 123-673) efficiently interacted with BCL6 (Fig. 5*B*, *lane 4*). The N-terminal end of the protein encompassing the first 122 amino acids as well as the deacetylase domain alone (674-1113) did not efficiently interact with BCL6 under the same conditions (Fig. 5*B*, *lanes 3* and *5*, respectively). We then precisely mapped the N-terminal BCL6-binding domain of HDAC5 using four smaller fragments covering this 123-673 region of interaction with BCL6 (Fig. 5*A*). This fine mapping allowed the identification of the region

123-292 of HDAC5 as the minimal interaction domain with BCL6 (Fig. 5*B*, *lanes 6-9*).

To evaluate the *in vivo* relevance of our *in vitro* interaction domain mapping, we examined the ability of different HDAC5 mutants to co-localize with BCL6 in cells by immunofluorescence analyses. Consistent with our mapping data, Fig. 5*C* shows that the N-terminal region of HDAC5 (*123-673*, *top panel*) almost systematically co-localized with BCL6, as did the full-length HDAC5. Under the same conditions, the isolated deacetylase domain (674-1113) showed no association with BCL6 in most of the cells (*middle panel*). Moreover, the *in vitro* defined "minimal" BCL6-binding site (HDAC5-(123-292), *bottom panel*) clearly kept the ability to co-localize with BCL6, albeit perhaps less efficiently than the HDAC5-(123-673) derivative.

Because both HDAC4 and HDAC7 share extensive sequence homology with HDAC5, and also associate with BCL6 *in vivo*, we investigated the possibility of an interaction between BCL6 and the N-terminal regions of HDAC4 and HDAC7. These two regions (HDAC4-(1-650) and HDAC7-(1-506)) were fused to GST and the purified proteins were indeed shown to associate with ^{35}S-labeled BCL6, whereas no binding was obtained with an equivalent amount of the GST protein alone (Fig. 5*D*). We concluded that BCL6 interacts with all the related class II HDACs *in vitro*.

Finally, a BCL6 minimal binding site in HDAC7 was also determined by GST pull-down. It showed that the most N-terminal domain of HDAC7-(1-254) efficiently interacted with the full-length BCL6 (Fig. 5*E*), whereas neither the histone deacetylase region (500-938) nor the central part of the protein (241-533) retained BCL6. A detailed analysis of the sequence of the minimal BCL6-interacting domain defined above showed it to encompass the most conserved region in the N-terminal non-deacetylase domain of HDAC4, -5, and -7 (not shown).

Delineation of the BCL6 Regions Involved in the Interaction with HDAC5-- Reciprocally, we next mapped the HDAC5-binding site of BCL6. To this end the ability of ^{35}S-BCL6 deletion mutants (Fig. 6*A*) to interact with GST-HDAC5-(123-673) was tested in GST pull-down assays. As expected, full-length BCL6 efficiently interacted with the HDAC5 N terminus in this assay (Fig. 6*B*, *panel 1*). Interestingly, BCL6 constructs lacking either the BTB/POZ domain (BCL6-(132-706), *panel 2*) or only containing the ZF region of the protein (BCL6-(501-706), *panel 3*) were able to associate with GST-HDAC5. Similar results were obtained with GST-HDAC7 (Fig. 6*C*, *panels 1-3*). These data pointed to an unexpected role for the ZF region in the recruitment of class II HDACs.

The BCL6 ZF region is composed of six C2-H2 *krüppel*-like zinc fingers (Fig. 6*A*, *fingers 1-6*). To further refine our mapping, BCL6 deletion mutants were prepared lacking 2, 4, or all the 6 ZFs. Removal of the two most C-terminal zinc fingers (fingers 5 and 6) did not significantly affect HDAC5 or HDAC7 binding (Fig. 6, *B* and *C*, *panel 4*). The additional deletion of the next two fingers (3 and 4) led to a drastic reduction in the capacity of BCL6 to interact with both HDAC5 and HDAC7 (BCL6 1-573, Fig. 6, *B* and *C*, *panel 5*). Fingers 3 and 4 therefore appear essential for the binding of these two histone deacetylases by BCL6. Moreover, the residual interaction observed in the total absence of zinc fingers is totally eliminated when the BTB/POZ domain was deleted (Fig. 6*B*, compare BCL6-(1-519) and -(132-519)), suggesting that the BTB/POZ domain represents also a minor site of interaction with HDAC5.

Although the *in vitro* data described above suggested a direct interaction between BCL6 and the class II HDACs, an indirect interaction because of the activity of proteins present in the reticulocyte lysates was possible. To rule out this possibility, we set up a baculovirus-based expression and purification of the ZF region of BCL6 (Fig. 6*D*, *left panel*). The purified protein was then incubated with purified bacterially expressed GST-HDAC5 fusions, containing or not the BCL6-binding sites, and immobilized on glutathione beads. The HDAC5 (123-292) region, shown to interact with BCL6 in reticulocyte lysate, efficiently interacted with the purified BCL6 ZF fragment as well (Fig. 6*D*, *right*, *upper panel*, *lane 3*). Under the same conditions, the fragment 451-673 of HDAC5 did not bind the BCL6 ZF, although equivalent amounts of GST fusion proteins were used in this assay (Fig. 6*D*, *right*, *lower panel*). These data clearly showed that the N-terminal region of HDAC5 can directly bind to the ZF region of BCL6.

To gain access to the *in vivo* relevance of these *in vitro* mapping, we tested the ability of different BCL6 constructs to recruit HDAC5 in cells. UTA-L cells were transiently co-transfected with HA-HDAC5 cDNA and plasmids encoding full-length BCL6 or mutants lacking either the two (BCL6-(1-626)) or the four C-terminal zinc fingers (BCL6-(1-573)). As expected, full-length BCL6 co-localized with HDAC5 in nuclear bodies and inclusions upon co-transfection (Fig. 6*E*, *top*). Interestingly, BCL6-(1-626) mostly localized in the cytoplasm, where it formed bodies retaining a large portion of the HDAC5 pool (Fig. 6*E*, *middle*). Surprisingly, the further removal of the two adjacent zinc fingers (BCL6-(1-573)) led to a diffuse distribution of the protein in the cytoplasm. In contrast to BCL6-(1-626), the BCL6-(1-573) derivative did not efficiently retain HDAC5 in the cytoplasm, as HDAC5 recovered its "usual" distribution, being predominantly observed in the nuclei of these cells (Fig. 6*E*, *bottom*).

Taken together, these data confirmed the results obtained *in vitro* as they showed the role of the N-terminal regions of both HDAC5 and -7, and of the ZF region of BCL6, as essential interaction interfaces in cells, and suggested that zinc fingers 3 and 4 of BCL6 are particularly involved in this interaction. The fact that the deletion of the regions necessary for the *in vitro* interaction, both in BCL6 or HDAC5, impaired their co-localization, is consistent with the idea that direct contacts are indeed important *in vivo* for the two proteins to associate. In addition, these results revealed that the last two zinc fingers of BCL6 are required for the nuclear targeting of this protein.

The Zinc Finger Region of BCL6 Mediates Transcriptional Repression-- Data presented above showed that the zinc finger region of BCL6 is involved in the recruitment of HDAC5 and HDAC7. It is therefore expected that the BCL6 ZF region repress transcription, when targeted to a promoter. To test this hypothesis, we targeted the BCL6 ZF region into a promoter containing GAL4-binding sites. The reporter system contained eight copies of the binding sites for LexA immediately adjacent to five copies of the binding site for GAL4, all cloned upstream from a luciferase gene (Fig. 7*A*). In the presence of LexA-VP16 fusion co-activator and the GAL4 DNA-binding domain alone (GAL4-DB), this reporter was activated to high levels of expression (Fig. 7*B*, *+LexA-VP16*). An expression vector was prepared expressing a fusion protein containing the ZF region of BCL6 (six fingers, amino acids 501-706) fused to the GAL4 DNA-binding domain. Co-expression of LexA-VP16 and GAL4-BCL6-(501-706) showed that the ZF region could efficiently inhibit the transcriptional activity of LexA-VP16 (Fig. 7*B*, *DB-BCL6 501-706* construct). Interestingly, the removal of the zinc fingers involved in the interaction with class II HDACs almost abolished the repressive effect of the domain. In control experiments, the expression of these GAL fusion

proteins had no effect on a promoter lacking the GAL4-binding site (Fig. 7*B*, *L8-Luc reporter*). Since the ZF region of BCL6 could efficiently recruit HDAC5 *in vitro* and *in vivo* (Fig. 6), we wanted to investigate the role of this HDAC activity in the ZF-mediated transcriptional repression described above. The same experiments as above were performed but cells were treated with HDAC inhibitor TSA 12 h before measurement of the luciferase activity. Surprisingly, the repressive activity of the ZF region of BCL6 was not abolished by TSA treatment, suggesting that, besides HDACs, other types of co-repressors could also participate in the repressive activity of this region of BCL6 (not shown).

Interaction of Class II HDACs with PLZF, Another POK Family Member-- Finally, we examined whether our observations could be extended to other (BTB/)POZ and *krüppel*-like zinc finger (POK) proteins. PLZF is another POK transcriptional repressor showing both functional similarities and association with BCL6 (Ref. 33 and references therein). Upon transient co-expression of both PLZF and class II HDACs in cells, an obvious co-localization of PLZF with HDAC4, -5, or -7 (Fig. 8*A*) was observed. Moreover, like BCL6, PLZF was able to interact directly with the N-terminal region of HDAC5, -4, and -7 in GST pull-down assays (Fig. 8*B*), suggesting that the class II HDACs interact with another POK factor at least and may therefore play a general role in regulating the function of these proteins.

Discussion

The data presented in this report show that BCL6 and PLZF harbor the capacity to recruit three related members of the class II HDACs, HDAC4, -5, and -7, and indicate that this recruitment relies, at least in part, on a direct interaction. A detailed investigation of these interactions revealed interesting properties of BCL6 and the studied HDACs.

BCL6-Zinc Finger Region Is a Multifunctional Domain-- Two domains of BCL6 are involved in the interactions with the class II HDACs: the N-terminal BTB/POZ domain and the C-terminal ZF region. A BCL6 derivative lacking the four C-terminal zinc fingers is severely impaired in its ability to bind HDAC5 and -7 *in vitro* and to co-localize with HDAC5 *in vivo*. Moreover, the deletion of both the entire ZF region and the BTB/POZ domain totally abrogates the interaction *in vitro*. Finally, the isolated ZF region of BCL6 is sufficient to directly interact with HDAC5 and -7 *in vitro*, and exhibits an autonomous repressive activity when targeted to a promoter *in vivo*. In addition to its already characterized DNA binding capacity, all these results suggest a role for the ZF region as an important heteromerization interface with class II HDACs. The ZF region of POK proteins therefore appears as a multifunctional domain, mediating specific interaction with DNA as well as with various protein partners, including class II HDACs. Indeed, the recruitment of a co-repressor by the C2-H2 zinc finger DNA-binding region of the CTCF transcription factor has been recently reported (40). Moreover, a deletion of the ZF region of the ZF5 POK protein has been shown to eliminate its ability to self-interact (41), whereas the ZF region of both BCL6 and PLZF were found to be involved in their heteromerization (33). Likewise, the ZF region of PLZF mediates its association with PML, the major translocation partner of RARα in acute promyelocytic leukemia (42, 43).

A Limited Region of HDAC4, -5, and -7 Targets Transcription Factors-- Regarding the BCL6-interacting region of class II HDACs, we identified their conserved non-catalytic N-terminal domain to be necessary and sufficient for the interaction with BCL6 *in vitro* and for co-localization in cells. This region is present in HDAC4, -5, and -7, as well as in the recently

cloned HDAC9 (26) and in MITR (44, 45), suggesting that these last two proteins probably also interact with BCL6. These data emphasize the importance of this domain in protein/protein interactions. Indeed, this domain has already been shown to bind MEF2 transcription factors as well as, at least for MITR, HDACs from both class I and class II and the CtBP co-repressor, indicating how the isolated HDAC5 N-terminal domain, or MITR, which lacks a catalytic deacetylase region, are capable of transcriptional repression (31, 44, 46). Moreover, this domain contains three conserved serines, two of them being possibly phosphorylated by the calcium/calmodulin-dependent protein kinases (CaMK). A regulated phosphorylation of these serines seems to control the interaction of these HDACs with partners as well as their intracellular localization (37, 47-52). Our data suggest that BCL6 may interfere with the nuclear/cytoplasmic shuttling of class II HDACs. For instance, HDAC4 appeared cytoplasmic in most cells when overexpressed "alone," but it became almost systematically detectable in the BCL6 nuclear bodies when overexpressed in induced UTA-L cells. Moreover, mapping experiments with either HDAC5 and -7 derivatives further indicated that the first half of their N-terminal domain is necessary and sufficient to bind BCL6. This highly conserved subregion also encompasses the binding site for the MEF2 transcription factors (31, 48, 49, 52-54). These findings suggest a cross-talk between BCL6 and the CaMK/HDACs/MEF2 pathway. Interestingly, like MEF2 transcription factors and presumably class II HDACs (39), BCL6 positively controls myogenesis as BCL6-deficient myocytes are more prone to undergo apoptosis upon serum withdrawal, possibly because they are impaired in their capacity to correctly arrest proliferation and/or to terminally differentiate (9).

BCL6 Recruits Multiple HDACs Directly or Indirectly-- HDAC4, -5, and -7 C-terminal regions bind silencing mediator of retinoid and thyroid receptors/nuclear receptor co-repressor (25, 55) and, at least for HDAC7, mSIN3A (25). All these co-repressors were previously found to also bind BCL6 (13, 16, 20). Moreover, B-CoR, a novel co-repressor interacting with the BCL6 BTB/POZ domain has been shown to associate with class II HDACs *in vivo* (22). Thus, BCL6 appears capable of interacting with class II HDACs both directly through its C-terminal ZF region (and to a lesser extent, its BTB/POZ domain) and indirectly by recruiting several co-repressors through its N-terminal half (16, 22). The possibility of multiple, direct, and indirect, contacts between BCL6 and class II HDACs parallels the situation of BCL6-class I HDACs interaction (16, 20). It could both confer more stability to the DNA-bound repressor complex(es) and increase the regulatory potential of the complex by broadening its linkage to distinct signaling pathways.

What Could Be the Role of the BCL6-HDACs Interaction?-- An obvious possibility for the role of BCL6-HDACs interaction is that BCL6 uses HDACs to exert transcriptional repression by local chromatin remodeling when targeted to specific promoters. It is also interesting to consider another hypothesis based on the ability of BCL6 and associated molecules to form specific "molecular reservoirs" allowing the assembly and reversible storage of class I and class II HDAC-containing regulatory complexes. In this respect, it is noteworthy that DNA replication has been found to progress on the periphery BCL6 nuclear core (35). BCL6-associated proteins could therefore be, at least in part, either deposited at specific promoters during DNA replication to maintain or alter the local chromatin structure, or involved in a broader function in chromatin maturation, especially the histone deacetylation that follows their association to the newly replicated DNA (56, 57). Finally, beyond the repression, another possibility would be that BCL6 could itself be a substrate of (at least some) its associated HDACs, which could thereby modulate its function. The report that the

acetyltransferase p300 may both acetylate BCL6 and regulate its repressive activity (58) provides support to this hypothesis.

Acknowledgements

We are grateful to Dr. J-J. Lawrence for encouraging this work, Dr. S. Rousseaux for the critical reading of the manuscript, Dr. M. Callanan for helpful discussion, and G. Géraud and C. Chamot (Service d'Imagerie of the Institut Jacques Monod, University of Paris VI/VII) for precious help in confocal microscopy analyses. We also thank S. Souquere-Besse, E. Pichard, and S. Curtet-Benitski for technical assistance, and M. Koken for the gift of the pSG5-PLZF expression vector and anti-PLZF antibody. Y. Kao wishes to thank Dr. R. Evans for support and encouragement. Part of this work has been carried out in R. Evan's laboratory.

Footnotes

* This work is supported by grants from CNRS, INSERM, Association pour la Recherche contre le Cancer (ARC), Ligue Nationale contre le Cancer and Groupement des Entreprises Françaises et Monégasques dans la lutte contre le Cancer (GEFLUC).The costs of publication of this article were defrayed in part by the payment of page charges. The article must therefore be hereby marked "*advertisement*" in accordance with 18 U.S.C. Section 1734 solely to indicate this fact.

‖James T. Pardee-Carl A. Gerstacker Assistant Professor of Cancer Research.

** Both authors contributed equally to this work.

To whom correspondence may be addressed. Tel.: 33-1-49-58-33-71; Fax: 33-1-49-58-33-81; E-mail: albagli@vjf.cnrs.fr.

§§ To whom correspondence may be addressed. Tel.: 33-4-76-54-95-74; Fax: 33-4-76-54-95-95; E-mail: khochbin@ujf-grenoble.fr.

Abbreviations

The abbreviations used are: HDAC, histone deacetylase; BCL6, B cell lymphomas 6; BTB/POZ, *bric à brac, tramtrack, broad complex/pox* virus and *z*inc finger; PLZF, promyelocytic leukemia zinc finger; GST, glutathione *S*-transferase; EM, electron microscopy; ZF, zinc finger; PBS, phosphate-buffered saline; HA, hemagglutinin.

References

1. Kerckaert, J.-P., Deweindt, C., Tilly, H., Quief, S., Lecocq, G., and Bastard, C. (1993) *Nat. Genet.* **5**, 66-70

2. Ye, B. H., Lista, F., Lo, Coco, F., Knowles, D. M., Offit, K., Chaganti, R. S., and Dalla-Favera, R. (1993) *Science* **262**, 747-750

3. Wales, M. M., Biel, M. A., el Deiry, W., Nelkin, B. D., Issa, J. P., Cavenee, W. K., Kuerbitz, S. J., and Baylin, S. B. (1995) *Nat. Med.* **1**, 570-577

4. Fujii, H., Biel, M. A., Zhou, W., Weitzman, S. A., Baylin, S. B., and Gabrielson, E. (1998) *Oncogene* **16**, 2159-2164

5. Reuter, S., Bartelmann, M., Vogt, M., Geisen, C., Napierski, I., Kahn, T., Delius, H., Lichter, P., Weitz, S., Korn, B., and Schwarz, E. (1998) *EMBO J.* **17**, 215-222

6. Dent, A. L., Shaffer, A. L., Yu, X., Allman, D., and Staudt, L. M. (1997) *Science* **276**, 589-592

7. Ye, B. H., Cattoretti, G., Shen, Q., Zhang, J., Hawe, N., de Waard, R., Leung, C., Nouri-Shirazi, M., Orazi, A., Chaganti, R. S., Rothman, P., Stall, A. M., Pandolfi, P. P., and Dalla-Favera, R. (1997) *Nat. Genet.* **16**, 161-170

8. Albagli, O., Dhordain, P., Lantoine, D., Auradé, F., Quief, S., Kerckaert, J.-P., Montarras, D., and Pinset, C. (1998) *Differentiation* **64**, 33-44

9. Kumagai, T., Miki, T., Kikuchi, M., Fukuda, T., Miyasaka, N., Kamiyama, R., and Hirosawa, S. (1999) *Oncogene* **18**, 467-475

10. Kojima, S., Hatano, M., Okada, S., Fukuda, T., Toyama, Y., Yuasa, S., Ito, H., and Tokuhisa, T. (2001) *Development* **128**, 57-65

11. Yoshida, T., Fukuda, T., Okabe, S., Hatano, M., Miki, T., Hirosawa, S., Miyasaka, N., Isono, K., and Tokuhisa, T. (1996) *Biochem. Biophys. Res. Commun.* **228**, 216-220

12. Shaeffer, A. L., Yu, X., He, Y., Boldrick, J., Chan, E. P., and Staudt, L. M. (2000) *Immunity* **13**, 199-212

13. Dhordain, P., Albagli, O., Lin, R. J., Ansieau, S., Quief, S., Leutz, A., Kerckaert, J.-P., Evans, R. M., and Leprince, D. (1997) *Proc. Natl. Acad. Sci. U. S. A.* **94**, 10762-10767

14. Hong, S. H., David, G., Wong, C. W., Dejean, A., and Privalsky, M. L. (1997) *Proc. Natl. Acad. Sci. U. S. A.* **94**, 9028-9033

15. David, G., Alland, L., Hong, S. H., Wong, C. W., DePinho, R. A., and Dejean, A. (1998) *Oncogene* **14**, 2549-2556

16. Dhordain, P., Lin, R., Quief, S., Kerckaert, J.-P., Evans, R. M., and Albagli, O. (1998) *Nucleic Acids Res.* **26**, 4645-4651

17. Guidez, F., Ivins, S., Zhu, J., Soderstrom, M., Waxman, S., and Zelent, A. (1998) *Blood* **91**, 2634-2642

18. Huynh, K. D., and Bardwell, V. (1998) *Oncogene* **17**, 2473-2484

19. Lin, R. J., Nagy, L., Inoue, S., Shao, W., Miller, W. H., Jr., and Evans, R. M. (1998) *Nature* **391**, 811-814

20. Wong, C. W., and Privalsky, M. L. (1998) *J. Biol. Chem.* **273**, 27695-27702

21. Wen, Y., Nguyen, D., Li, Y., and Lai, Z. C. (2000) *Genetics* **156**, 195-203

22. Huynh, K. D., Fischle, W., Verdin, E., and Bardwell, V. J. (2000) *Genes Dev.* **14**, 1810-1823

23. Verdel, A., and Khochbin, S. (1999) *J. Biol. Chem.* **274**, 2440-2445

24. Grozinger, C. M., Hassig, C. A., and Schreiber, S. L. (1999) *Proc. Natl. Acad. Sci. U. S. A.* **96**, 4868-4873

25. Kao, H.-Y., Downes, M., Ordentlich, P., and Evans, R. M. (2000) *Genes Dev.* **14**, 55-66

26. Zhou, X., Marks, P. A., Rifkind, R. A., and Richon, V. M. (2001) *Proc. Natl. Acad. Sci. U. S. A.* **98**, 10572-10577

27. Kao, H.-Y., Lee, C. H., Komarov, A., Han, C. C., and Evans, R. M. (2002) *J. Biol. Chem.* **277**, 187-193

28. Fisher, D. D., Cai, R., Bhatia, U., Asselbergs, F. A. M., Song, C., Terry, R., Trogani, N., Widmer, R., Atadja, P., and Cohen, D. (2002) *J. Biol. Chem.* **277**, 6656-6666

29. Guardiola, A. R., and Yao, T.-P. (2002) *J. Biol. Chem.* **277**, 3350-3356

30. Khochbin, S., Verdel, A., Lemercier, C., and Seigneurin-Berny, D. (2001) *Curr. Opin. Genet. Dev.* **11**, 162-166

31. Lemercier, C., Verdel, A., Galloo, B., Curtet, S., Brocard, M. P., and Khochbin, S. (2000) *J. Biol. Chem.* **275**, 15594-15599

32. Lemercier, C., To, R. Q., Carrasco, R. A., and Konieczny, S. F. (1998) *EMBO J.* **17**, 1412-1422

33. Dhordain, P., Albagli, O., Honoré, N., Guidez, F., Lantoine, D., Schmid, M., de Thé, H., Zelent, A., and Koken, M. H. M. (2000) *Oncogene* **19**, 6240-6250

34. Albagli, O., Lantoine, D., Quief, S., Quignon, F., Englert, C., Kerckaert, J.-P., Montarras, D., Pinset, C., and Lindon, C. (1999) *Oncogene* **18**, 5063-5075

35. Albagli, O., Lindon, C., Lantoine, S., Quief, S., Puvion, E., Pinset, C., and Puvion-Dutilleul, F. (2000) *Mol. Cell. Biol.* **20**, 8560-8570

36. Chang, C. C., Ye, B. H., Chaganti, R. S., and Dalla-Favera, R. (1996) *Proc. Natl. Acad. Sci. U. S. A.* **93**, 6947-6952

37. McKinsey, T. A., Zhang, C. L., Lu, J., and Olson, E. N. (2000) *Nature* **408**, 106-111

38. Miska, E. A., Langley, E., Wolf, D., Karlsson, K., Pines, J., and Kouzarides, T. (2001) *Nucleic Acids Res.* **29**, 3439-3447

39. Zhao, X., Ito, A., Kane, C. D., Liao, T-S., Bolger, T. A., Lemrow, S. M., Means, A. R., and Yao, T-P. (2001) *J. Biol. Chem.* **276**, 35042-35048.

40. Lutz, M., Burke, L. J., Barreto, G., Goeman, F., Greb, H., Arnold, R., Schultheiss, H., Brehm, A., Kouzarides, T., Lobanenkov, V., and Renkawitz, R. (2000) *Nucleic Acids Res.* **28**, 1707-1713

41. Numoto, M., Yokoro, K., and Koshi, J. (1999) *Biochem. Biophys. Res. Commun.* **256**, 573-578

42. Koken, M. H., Reid, A., Quignon, F., Chelbi-Alix, M. K., Davies, J. M., Kabarowski, J. H., Zhu, J., Dong, S., Chen, S., Chen, Z., Tan, C. C., Licht, J., Waxman, S., de The, H., and Zelent, A. (1997) *Proc. Natl. Acad. Sci. U. S. A.* **94**, 10255-10260

43. Melnick, A., and Licht, J. D. (1999) *Blood* **93**, 3167-3215

44. Sparrow, D. B., Miska, E. A., Langley, E., Reynaud-Deonauth, S., Kotecha, S., Towers, N., Spoh, G., Kouzarides, T., and Mohun, T. (1999) *EMBO J.* **18**, 5085-5098

45. Zhou, X., Richon, V. M., Rifkind, R. A., and Marks, P. A. (2000) *Proc. Natl. Acad. Sci. U. S. A.* **97**, 1056-1061

46. Zhang, C. L., McKinsey, T. A., Lu, J., and Olson, E. N. (2001) *J. Biol. Chem.* **276**, 35-39

47. Wang, A. H., Kruhlak, M. J., Wu, J., Bertos, N. R., Vezmar, M., Posner, B. I., Bazett-Jones, D. P., and Yang, X. J. (2000) *Mol. Cell. Biol.* **20**, 6904-6912

48. Lu, J., McKinsey, T. A., Nicol, R. L., and Olson, E. N. (2000) *Proc. Natl. Acad. Sci. U. S. A.* **97**, 4070-4075

49. Lu, J., McKinsey, T. A., Zhang, C. L., and Olson, E. N. (2000) *Mol. Cell.* **6**, 233-244

50. McKinsey, T. A., Zhang, C. L., Lu, J., and Olson, E. N. (2000) *Proc. Natl. Acad. Sci. U. S. A.* **97**, 14400-14405

51. Grozinger, C. M., and Schreiber, S. L. (2000) *Proc. Natl. Acad. Sci. U. S. A.* **97**, 7835-7840

52. Kao, H.-Y., Verdel, A., Tsai, C. C., Simon, C., Juguilon, H., and Khochbin, S. (2001) *J. Biol. Chem.* **276**, 47469-47507

53. Wang, A. H., Bertos, N. R., Vezmar, M., Pelletier, N., Crosato, M., Heng, H. H., Th'ng, J., Han, J., and Yang, X. J. (1999) *Mol. Cell. Biol.* **19**, 7816-7827

54. Miska, E. A., Karlsson, C., Langley, E., Nielsen, S. J., Pines, J., and Kouzarides, T. (1999) *EMBO J.* **18**, 5099-5107

55. Huang, E. Y., Zhang, J., Miska, E. A., Guenther, M. G., Kouzarides, T., and Lazar, M. A. (2000) *Genes Dev.* **14**, 45-54

56. Krude, T. (1995) *Exp. Cell Res.* **220**, 304-311

57. Tyler, J. K., Bulger, D. M., Kamakaka, R. T., Kobayashi, R., and Kadonaga, J. T. (1996) *Mol. Cell. Biol.* **16**, 6149-6159

58. Bereshchenko, O. R., Gu, W., and Dalla-Favera, R. (2000) *Blood* **96**, 702a (Abst. 3028)

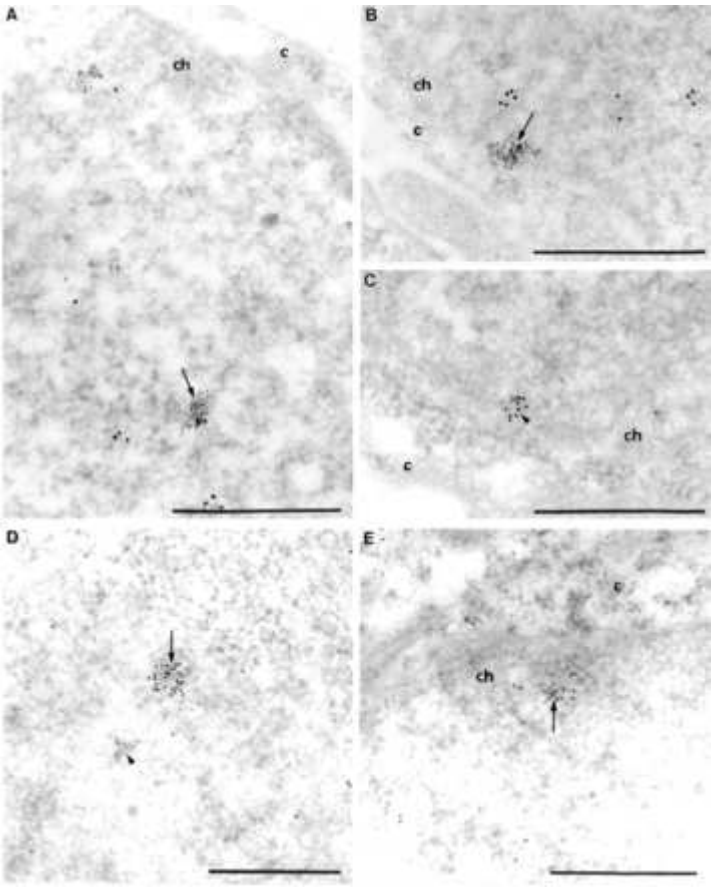

Fig. 1. Partial co-localization of endogenous BCL6 and endogenous class II HDACs in human A549 lung cells and mouse C2 myocytes. Immunogold labeling and electron microscopy were used to co-detect BCL6 and HDAC4 in A549 (*A* and *B*) and C2 (*C*) cells. The 6-nm gold particles, which localize BCL6, are scattered through the nucleus or constitute aggregates up to 100 nm in diameter. HDAC4, which is revealed by the 12-nm gold particles, mainly appeared as isolated or small groups of gold particles. The *arrows* point to BCL6 aggregates with enclosed HDAC4 molecules in A549 cells. These co-localization foci are located either in the interior of the nucleus (in *A*) or at the nuclear border (in *B*). The *arrowhead* in *C* points to a cluster of 12-nm particles (HDAC4) juxtaposed to a cluster of 6-nm particles (BCL6) in C2 cells. *D* and *E*, co-detection of BCL6 and HDAC5 in A549 cells. In *D*, the 12-nm gold particles which localize HDAC5 are scattered through the cell or accumulated over a dot (*arrow*), about 150 nm in diameter, which is devoid of 6-nm gold particles, the latter constituting an independent aggregate (*arrowhead*). In *E*, the *arrow* points to juxtaposed clusters of 6- and 12-nm gold particles located at the nuclear border. *c*, cytoplasm; *ch*, perinuclear layer of condensed chromatin. *Bars*, 0.5 μm.

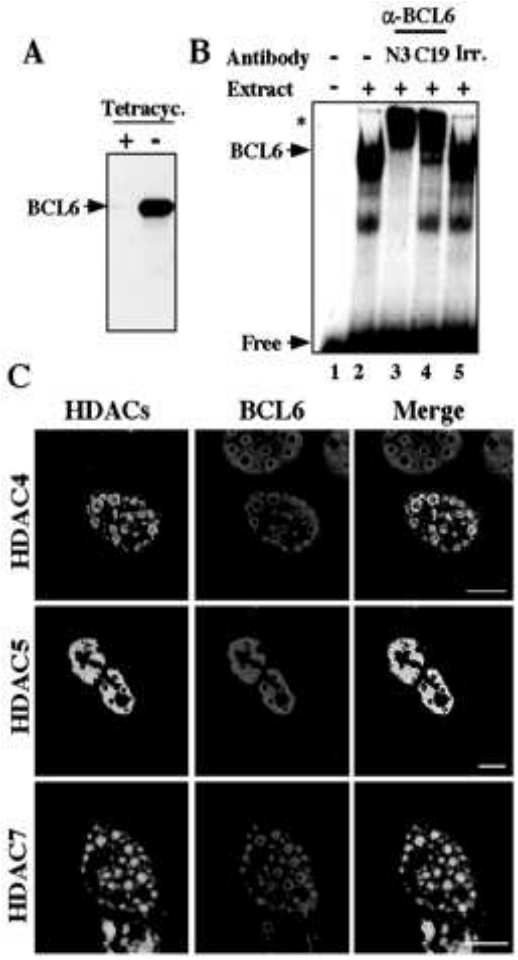

Fig. 2. Co-localization of HDAC4, HDAC5, and HDAC7 with BCL6 in a BCL6-inducible stably transfected cell line. *A*, total cell extracts were prepared from BCL6 UTA-L stably transfected cells grown in the presence (+, non-induced) or absence (−, induced) of tetracycline for 24 h. BCL6 expression was detected by Western blotting using anti-BCL6 C19 antibody. *B*, overexpressed BCL6 binds to a BCL6-DNA target sequence: electrophoretic mobility shift assay analysis. Cell extracts were prepared from induced UTA-L cells and incubated with a ^{32}P-labeled oligonucleotide containing a BCL6-binding site (*lanes 2-5*). A supershift (denoted by an *asterisk*) is observed in the presence of anti-BCL6 N3 (*lane 3*) or C19 (*lane 4*) antibodies but not in the presence of an irrelevant antibody (*lane 5*). *Lane 1* contains only the labeled probe. *C*, co-localization of class II HDACs with BCL6 in UTA-L cells. HA-HDAC4 (*top*), -5 (*middle*), or -7 (*bottom*) were transfected in BCL6 expressing UTA-L cells. Cells were then subjected to a double staining using the polyclonal Y11 anti-HA (*green*) and mouse monoclonal M2 anti-Flag (*red*) antibodies to detect HDACs and BCL6, respectively, using confocal microscopy. *Bars*, 10 μm.

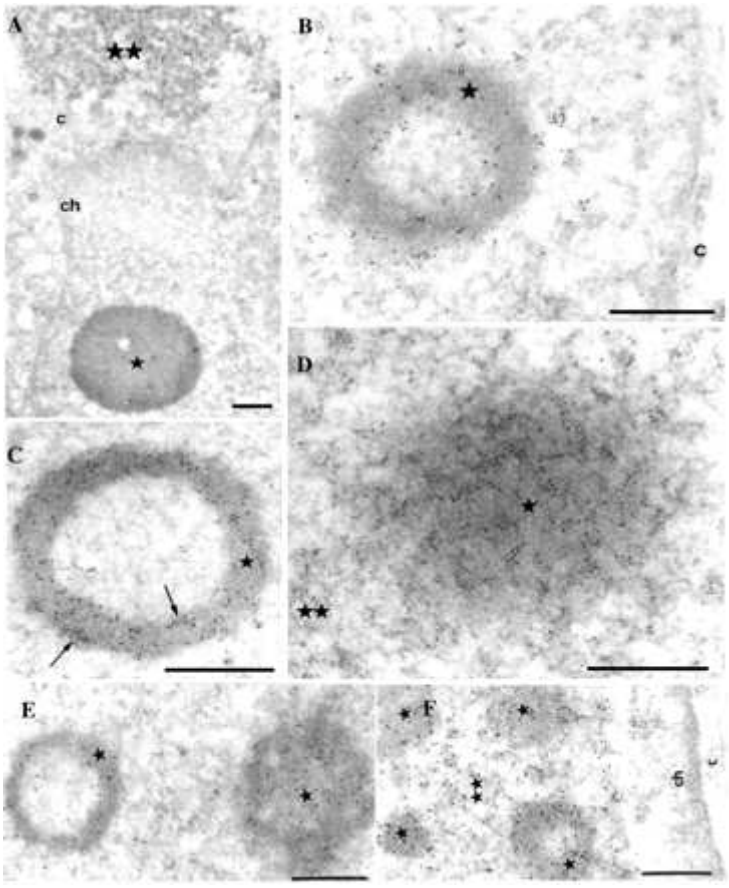

Fig. 3. Ultrastructural analysis of BCL6 and class II HDACs co-localization. Induced (BCL6 expressing) cells were transfected with vector encoding HA-HDAC4 (*A* and *B*), HA-HDAC5 (*C* and *D*), and HA-HDAC7 (*E* and *F*) as in Fig. 2*C*, and prepared for EM analysis using the Y11 anti-HA or either the M2 anti-Flag or C19 anti-BCL6 antibody to detect class II HDACs and BCL6, respectively. *A*, the anti-HA antibody (10-nm gold particles) stained both a cytoplasmic inclusion near to the nucleus (*double star*) and a typical, morphologically well identifiable, nuclear BCL6 bodies (*star*). *B*, sometimes, HDAC4 antibody (10-nm gold particles) is also detected in the interior and in the surrounding nucleoplasm of the BCL6 bodies (*star*). *C*, HA-HDAC5 antibody (5-nm gold particles, see *arrow*) is both present onto, as well as within, a nuclear BCL6 body (*star*) stained by 10-nm gold particles. *D*, upon higher HDAC5 expression, large nuclear inclusions (*double star*) embedding the BCL6 bodies (*star*) were found. Both the inclusions and the embedded BCL6 bodies were co-stained with the anti-HA (10-nm gold particles) and the anti-Flag (5-nm gold particles) antibodies demonstrating the complete co-distribution of the two proteins. *E* and *F*, similarly, HDAC7 (10-nm gold particles) was either recruited onto free BCL6 nuclear bodies (*E*, *stars*) or formed inclusions (*F*, *double star*) enclosing BCL6 bodies (star). *c*, cytoplasm; *ch*, condensed chromatin. *Bars*, 0.5 μm.

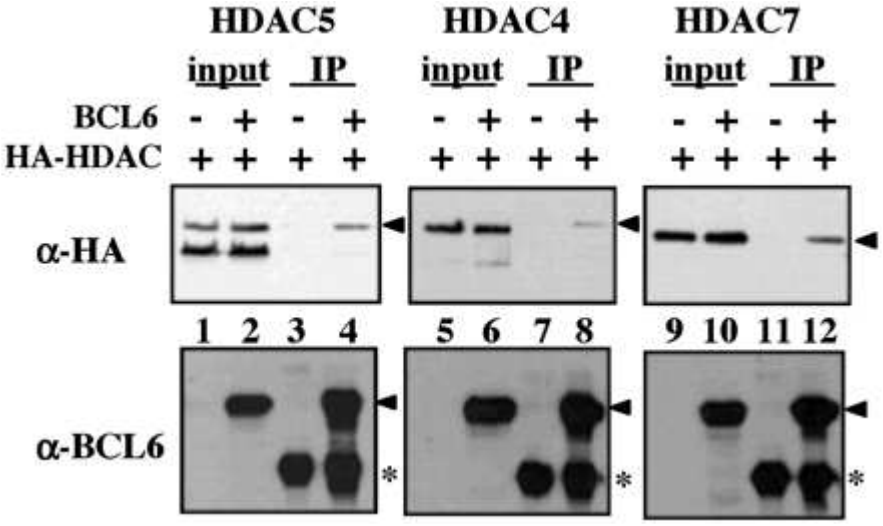

Fig. 4. BCL6 forms stable complexes with class II HDACs *in vivo*. UTA-L cells were transfected with pcDNA-HA-HDACs vectors (HDAC5, -4, or -7) and pcDNA-BCL6 or the empty pcDNA3.1 plasmid. Thirty-six hours after transfection, cells were collected and submitted to immunoprecipitation with an anti-BCL6 antibody. The immunoprecipitated materials were analyzed by Western blotting using an anti-HA antibody to detect the HA-HDACs proteins as indicated (*upper panels*) or the anti-BCL6 antibody (*lower panels*). Input lanes correspond to an aliquot of the soluble proteins before the immunoprecipitation step. *Asterisks* represent the Ig band. The *arrowheads* indicate the full-length protein.

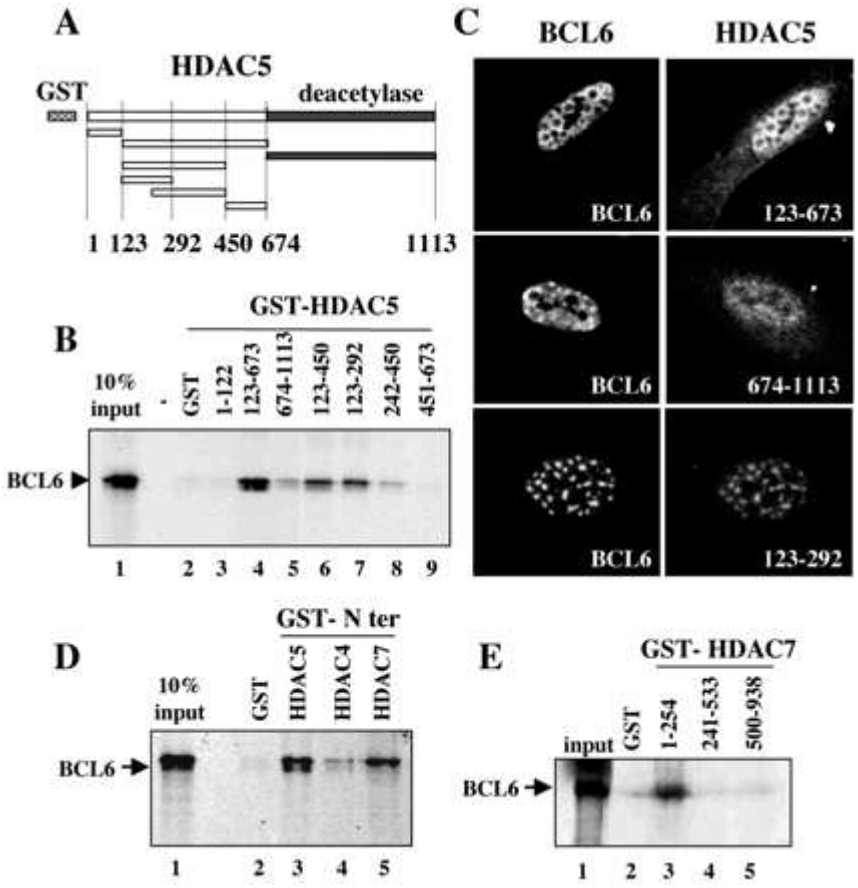

Fig. 5. BCL6 interacts with the N-terminal domain of the class II HDACs *in vitro*. *A*, schematic representation of GST-HDAC5 fragments used in this study; *B*, GST alone or the indicated GST-HDAC5 proteins immobilized on glutathione-agarose beads were incubated with full-length ^{35}S-labeled BCL6. After the pull-down, the bound proteins were resolved by SDS-PAGE and submitted to autoradiography. *C*, deletion of the N-terminal region of HDAC5 impairs its co-localization with BCL6 *in vivo*. Induced UTA-L (BCL6 expressing) cells were transiently transfected with the HA-HDAC5-(123-673) (*top*); HA-HDAC5-(674-113) (*middle*) and HA-HDAC5-(123-292) (*bottom*). BCL6 and HA-HDAC5 derivatives were detected with M2 anti-Flag and Y11 anti-HA antibodies, respectively. *D*, GST pull-down was performed as in *B* with GST-HDAC5-(123-673), GST-HDAC4-(1-650), and GST-HDAC7-(1-506), and ^{35}S-labeled BCL6. *E*, mapping of the HDAC7 region involved in the binding to BCL6. A pull-down was performed as in *B* with the indicated GST-HDAC7 fragments and full-length ^{35}S-labeled BCL6.

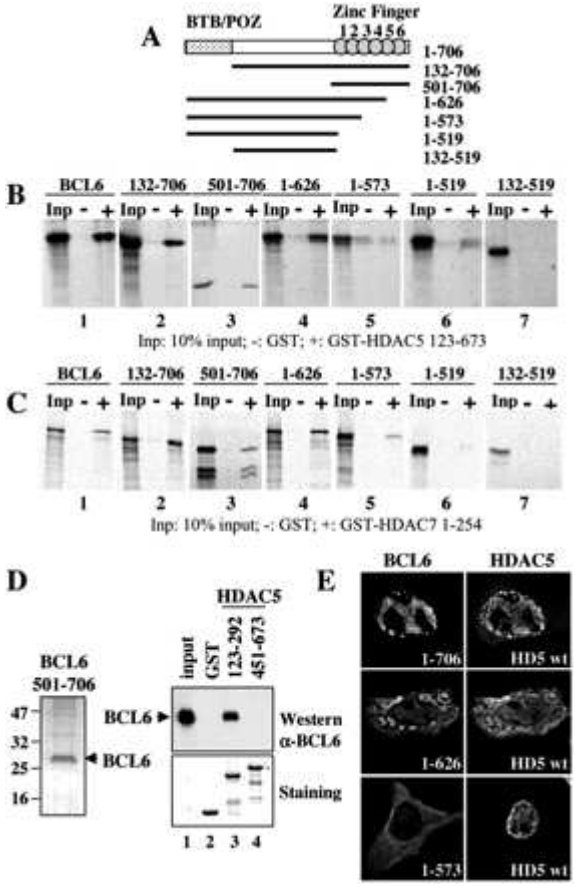

Fig. 6. Mapping of the BCL6 regions involved in the interaction with HDAC5 and HDAC7. *A*, schematic representation of the BCL6 deletion fragments tested. ^{35}S-Labeled BCL6 proteins were incubated with GST-HDAC5-(123-673) (*B*) or GST-HDAC7-(1-254) (*C*) immobilized on glutathione-agarose beads (+ *lanes*) or GST protein alone (− *lanes*). The bound proteins were resolved by SDS-PAGE and detected by autoradiography. *Inp*, input of ^{35}S-labeled protein. *D*, direct interaction between the ZF region of BCL6 and HDAC5-(123-292). A baculovirus expression system was setup to express and purify the ZF region of BCL6 (*left*, Coomassie Blue staining). The purified BCL6 ZF region was then used in pull-down experiments with the indicated region of HDAC5 fused to GST and immobilized on glutathione beads. The bound BCL6 ZF region was detected by Western blotting using an anti-BCL6 antibody (*top right*). The Coomassie panel shows the amount of GST fusion protein used in this assay (*bottom right*). Input lane shows 10% of the BCL6 ZF fragment used in the pull-down assays. *E*, UTA-L cells were co-transfected with a HA-HDAC5 expression vector plus a vector encoding either wild-type BCL6 (*top*) or a BCL6 derivatives lacking either the two last zinc fingers (BCL6-(1-626), *middle*) or the four last zinc fingers (BCL6-(1-573), *bottom*). Wild type and mutants BCL6 and HA-HDAC5 were detected with polyclonal N3 anti-BCL6 and rat 3F10 anti-HA antibodies, respectively.

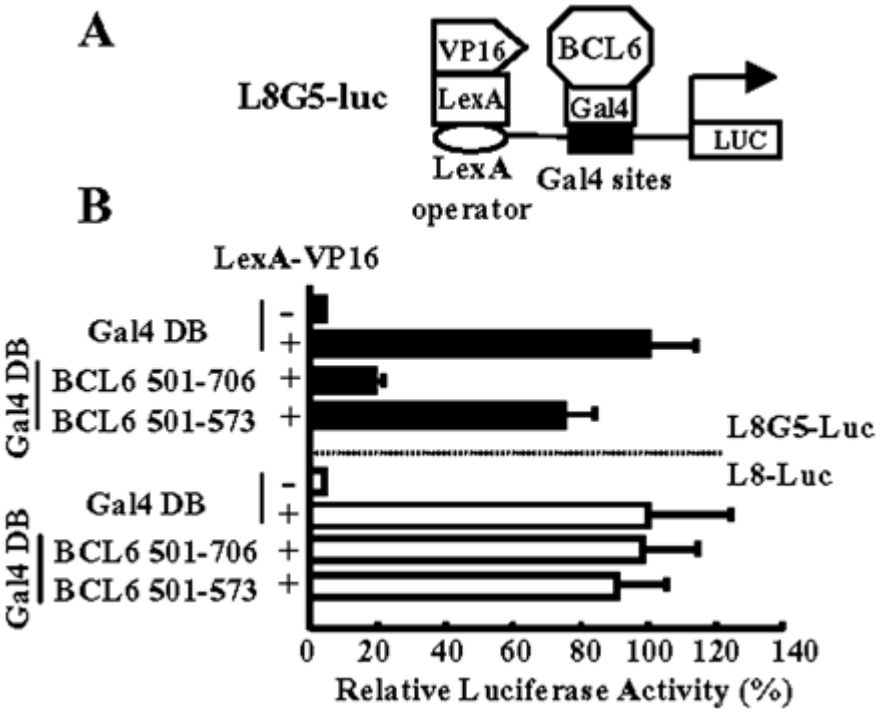

Fig. 7. The isolated zinc finger region of BCL6 mediates transcriptional repression. *A*, schematic representation of L8G5-luc reporter system. *B*, HeLa cells were transfected with 400 ng of L8G5-Luc reporter (*black bars*) and 20 ng of vectors expressing either the Gal4 DNA-binding domain alone (*DB*) or the indicated Gal4 DB-BCL6 fusion proteins, in the presence of 100 ng of LexA-VP16 activator plasmid. In a control experiment, L8G5-Luc was substituted by L8-Luc reporter lacking Gal4 DNA-binding sites (*white bars*). Luciferase activity obtained from L8G5-Luc plasmids in the presence of Gal4-DB is set at 100%. Mean ± S.D. of at least three independent transfections.

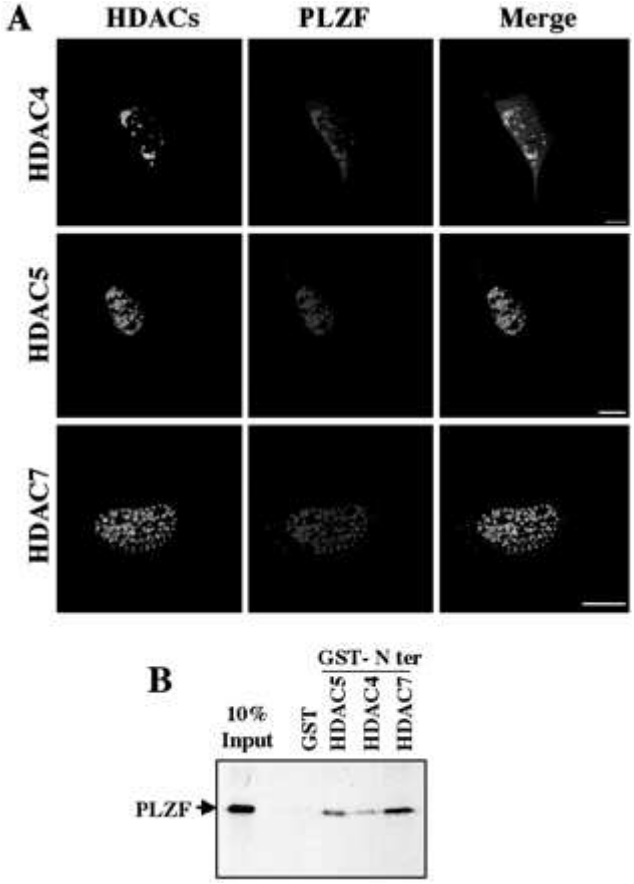

Fig. 8. HDAC 4, -5, and -7 co-localize and interact with PLZF. *A,* mouse C2 cells were co-transfected with a PLZF expression vector together with expression vectors encoding HA-HDAC4, -5, or -7. Cells were fixed 24 h after transfection and analyzed by immunofluorescence using the Y11 anti-HA antibody (*green*) and a monoclonal anti-PLZF antibody (*red*) and confocal microscopy. *Bars*, 20 μm. *B,* GST pull-down assays were performed as described in the legend to Fig. 5*D* using full-length ^{35}S-labeled PLZF and GST-HDAC5-(123-673), -HDAC4- (1-650), and -HDAC7-(1-506).